Hindawi Publishing Corporation
Advances in Condensed Matter Physics
Volume 2013, Article ID 373079, 7 pages
http://dx.doi.org/10.1155/2013/373079

Research Article

Phase Relations in $Ba_{6-3x}Ln_{8+2x}Ti_{18}O_{54}$ (Ln = Nd & Sm) Electroceramics

Amanda L. Snashall,[1] Yun Liu,[1] Frank Brink,[2] Ray L. Withers,[1] and Steven Cooper[3]

[1] *Research School of Chemistry, Australian National University, Acton, Australian Capital Territory 0200, Australia*
[2] *Centre for Advanced Microscopy, Australian National University, Acton, Australian Capital Territory 0200, Australia*
[3] *Mesaplexx Pty. Ltd., 31 Kurilpa Street, West End, Brisbane, Queensland 4101, Australia*

Correspondence should be addressed to Yun Liu; yliu@rsc.anu.edu.au

Received 31 May 2013; Accepted 28 July 2013

Academic Editor: Danyang Wang

A careful, systematic investigation of $Ba_{6-3x}Ln_{8+2x}Ti_{18}O_{54}$ (BLnTss) ceramics has been performed in order to understand the relationship between composition, microstructure evolution, and microwave dielectric properties. In this paper, we report the effects of composition, morphology, and sintering time on the phase relations and properties of BLnTss (Ln = Nd, Nd/Sm, Sm) ceramics. The microwave dielectric properties of the materials are reported in addition to phase characterisation and structural analysis via X-ray diffraction and field emission scanning electron microscopy coupled with energy dispersive X-ray spectroscopy. BLnTss, $x = 0.33$, ceramics with high Sm content are found to experience a severe degradation of Qf and changes in τ_{cf} trending, associated with the onset of globular and needle-like grain morphology and a Ba-Ti rich phase. $x = 0.67$ ceramics with high Nd content are found to exhibit a secondary phase ($Nd_2Ti_2O_7$) upon prolonged sintering which resulted in beneficial changes to Qf and τ_{cf} without affecting ε_r. Two BLnTss ceramics compositions with near-zero τ_{cf} were successfully synthesised with high Qf and ε_r values.

1. Introduction

Dielectric ceramics are fundamental building blocks of modern microwave telecommunications technology, being widely used as resonators in filters, phase shifters, and dielectric resonator antennas [1]. $Ba_{6-3x}Ln_{8+2x}Ti_{18}O_{54}$ solid solutions (BLnTss, Ln = lanthanide) in ceramic form have attracted significant interest since their discovery in 1968 [2] and subsequent investigation in 1981 [3] due to their high dielectric permittivity (ε_r), comparatively high quality factor (Qf), and moderate temperature coefficient of resonant frequency (τ_{cf}) at microwave frequencies [4].

The tungsten bronze-type structure of these BLnTss ceramics is composed of corner sharing blocks of TiO_6-octahedra of perovskite-like structure. These perovskite-like blocks are in turn corner-connected to one another leading to three distinct potential locations for Ba and Ln cation insertion, forming channels running parallel to the *b*-axis; 12-coordinate rhombohedral sites (A1-sites within the perovskite-like block regions) preferentially occupied by Ln^{3+} cations, 15-coordinate pentagonal sites (A2-sites) preferentially filled with Ba^{2+}, and 9-coordinate trigonal sites (C-sites) that remain vacant due to their restrictive size [5]. In order to form the upper limit of the $Ba_{6-3x}Ln_{8+2x}Ti_{18}O_{54}$ solid solution, Ba^{2+} substitutes for Ln^{3+} and vacancies on A1-sites, while the lower limit of the solid solution is determined by excessive vacancy formation in the A1- and A2-sites which destabilises the BLnTss structure. The dielectric properties of BLnTss ceramics vary substantially with the Ba/Ln ratio as well as with the selection of the lanthanide, as each results in a distortion of the ideal structure and its resultant properties [6]. BLnTss ceramics with Ln = La, Pr, and Nd have been reported to display a positive τ_{cf} while Ln = Sm, Eu, and Gd display negative τ_{cf} [5]. BLnTss compounds combining lanthanides with opposite τ_{cf} characteristics have been found

to form a final product with a near-zero τ_{cf} when mixed in correct proportions [7], resulting in high commercial demand for compounds of this type [8].

It is noteworthy that the BLnTss system does not have a well-defined crystallisation temperature [9] and its X-ray diffraction patterns are rather too complicated to determine the phase composition, with common secondary phases "masked" by superposition of main diffraction peaks. As a result, there is some uncertainty surrounding the solid solubility limits for both the Ln = Sm and Ln = Nd analogues of $Ba_{6-3x}Ln_{8+2x}Ti_{18}O_{54}$ [9]. In this paper we report the effects of composition, sintering temperature, and time on the properties of BLnTss (Ln = Nd, Sm, and Nd-Sm) ceramics. A careful, systematic investigation is performed to build a relationship between composition, microstructure evolution, and microwave dielectric properties. This investigation, particularly, focuses on changes in morphology and the effects of prolonged annealing, which had previously been shown to result in unexplained cell parameter and dielectric properties variation deserving of further attention [10].

2. Materials and Methods

$Ba_{6-3x}(Nd_{1-y}Sm_y)_{8+2x}Ti_{18}O_{54}$ electroceramics were synthesized via solid state reaction using $BaCO_3$ (>2N, May and Baker), Nd_2O_3 (3N, Pi-KEM), Sm_2O_3 (3N, Pi-KEM), and TiO_2 (4N, PiKEM, 20 nm). The reported solid solution range of BLnTss (Ln = Sm, Nd) compounds is approximately $0.25(5) \leq x \leq 0.75(5)$ [8, 11–13]; therefore the compositions investigated in this paper were $x = 0.33, 0.5, 0.67$, henceforth referred to as compositions A, B, and C, respectively. To observe the effects of varying the size of the lanthanide, for each composition A, B, and C, samples for $y = 0$, 0.2, 0.4, 0.6, 0.8, and 1 were synthesised, henceforth referred to as A0, A2, A4, and so forth. All starting materials were thoroughly dried prior to weighing, with Nd_2O_3 and Sm_2O_3 undergoing an additional high temperature (1000°C) treatment prior to weighing to minimise stoichiometric errors due to the formation of $Ln_xO_y(OH)_{3x-2y}$.

Reagents were mixed in appropriate ratios, ball-milled for 12 hours under ethanol (polyoxymethylene canisters, stabilised ZrO_2 balls) and then dried in an oven to vaporise residual milling solvent. These powders were then sieved to a particle size <125 μm and calcined at 1100°C for 4 hours in air. Individual cylindrical samples were formed via 5 tonne anisotropic pressing using polyvinyl alcohol as a binding agent. Batches of each composition were subsequently sintered at temperatures between 1250 and 1375°C on platinum foil within an alumina crucible. To promote solid-state reaction characteristics and mitigate potential compositional variation effects, nanoscale TiO_2 was used as a starting reagent, and a minimum sintering period of 4 hours was selected [14, 15]. The optimum sintering temperature was found to be 1375°C with samples of each composition sintered for 4 hours (e.g., A0-4) and 60 (e.g., A0-60) hours to observe the effects of prolonged heat treatment. Densification was determined via the Archimedes method.

Phase composition was investigated via XRD (Siemens D-5000). Field emission scanning electron microscopy (FESEM) was used to characterise both morphology (Zeiss UltraPLus FESEM) and phase distribution (Hitachi 4300SE/N FESEM). Quantitative analyses were undertaken via electron probe microanalysis (EPMA on Hitachi: 15 kV, 600 pA) with $Nd_2Ti_2O_7$, SmP_5O_{14}, and $BaSO_4$ used as calibration standards.

A network analyser (Agilent E5062A) was used to characterise microwave dielectric properties based on the TE_{011} resonant mode. Q values were calculated using "QZERO for Windows". The dielectric constant (ε_r) was obtained using a 3D finite element analysis (FEA) *eigenmode* solver. The temperature coefficient of resonant frequency (τ_{cf}) was calculated via the relation $\tau_{cf} = \Delta f / f \Delta T$ (ppm/K).

3. Results and Discussion

All A-Series samples were initially identified as single phase via XRD. Sintered surface morphology displayed a significant increase in density with prolonged sintering time (Figures 1(a) and 1(b)) and increasing Sm content (Figures 1(a), 1(c), and 1(d)). All A-series samples displayed the formation of columnar-type grains characteristic of BLnTss ceramics, in good agreement with previous reports [9, 10]. Smooth "globular" shaped grains (indicated in Figure 1(c)) were evident in A-series samples with $y \geq 0.4$, and needle-like characteristics were observed for some grains within the $y = 1.0$ sample (as indicated in Figure 1(d)). SEM backscatter imaging displayed distinct differential contrast between the columnar grains typical of BLnTss and the needle-like grains observed for A10-4 (Figure 1(e)) and A10-60, indicating the presence of a secondary phase.

EPMA compositional analysis of both the main phase and the contrasting phase was undertaken on the "as-sintered" surface of the A10-60 sample. Due to the restrictive grain size of the darker contrast regions, an exact composition could not be determined; however these areas indicated increased levels of Ba and Ti and a significant reduction in Sm content when compared with the main phase (Table 1 (a)-(b)). In order to better identify the phase nature of the needle-type morphology grains, the A10-60 sample was polished and reexamined.

When polished, there was no detectable secondary phase in the A10-60 sample at low-to-medium magnification, with spot and area analyses confirming the nominal stoichiometry within the limits of experimental error. At high magnification, FESEM images were compared with the corresponding backscattered images (Figure 2(a)), to reveal darker patches almost indistinguishable at maximum backscatter detector contrast. Due to their small surface area, EPMA quantitative analysis of these darker areas was not feasible; however spot analysis (Table 1 (c)-(d)) concentrated on such grain regions and surface mapping (Figures 2(b)–2(d)) of the sample revealed the existence of regions rich in Ba and Ti, with reduced Sm content when compared to the main phase. These results, in good agreement with the EPMA compositional analysis of the as-sintered surface, indicate the presence of

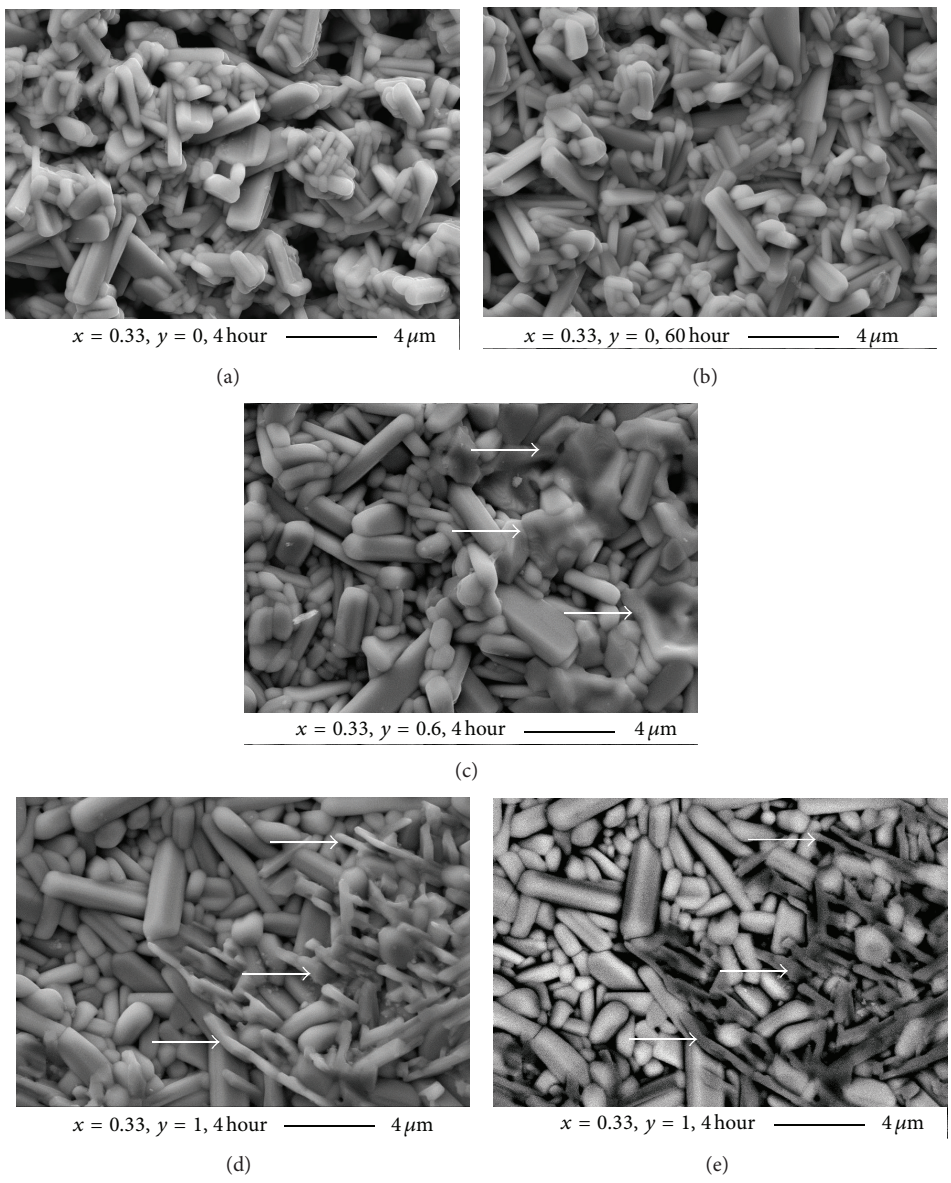

Figure 1: SEM images of $x = 0.33$ samples sintered at 1375°C for either 4 or 60 hours. Secondary electron images of (a) A0-4, (b) A0-60, (c) A6-4, and (d) A10-4 and matching backscattered electron images for (e) A10-4.

Table 1: EPMA quantitative results for A10-60 sample, for "as-sintered" (a, b) and polished surfaces (c, d).

Area under analysis	Surface type	Ba [At. %]	Sm [At. %]	Ti [At. %]
(a) Column-like (BSE lighter)	As-sintered	5.72 (9)	10.36 (13)	20.89 (16)
(b) Needle-like morphology (BSE darker)*	As-sintered	8.29 (11)	3.55 (51)	24.85 (37)
(c) BSE light contrast region	Polished	5.68 (14)	10.20 (12)	21.05 (10)
(d) BSE dark contrast region*	Polished	12.49 (1.19)	5.21 (74)	20.66 (18)

*Analysis represents a composite of the main phase and the dark contrast region due to restrictive grain size.

a Ba/Ti-rich secondary phase, either extremely poor in or completely devoid of Sm, and not previously reported for this composition. This secondary phase was unable to be further defined, as grain size limited the effectiveness of EPMA analysis, while the complex nature of the main phase X-ray diffraction pattern concealed this Bi/Ti-rich secondary phase.

Figure 3(a) presents the microwave dielectric properties of the A-series samples. For $y = 1$, both the A10-4 and A10-60 samples were found to correlate well with the reported dielectric properties for single-phase Sm-BLnTss, with an extremely low Qf, a moderate ε_r, and a highly negative τ_{cf} measured [16]. The Qf and τ_{cf} of the A-Series samples

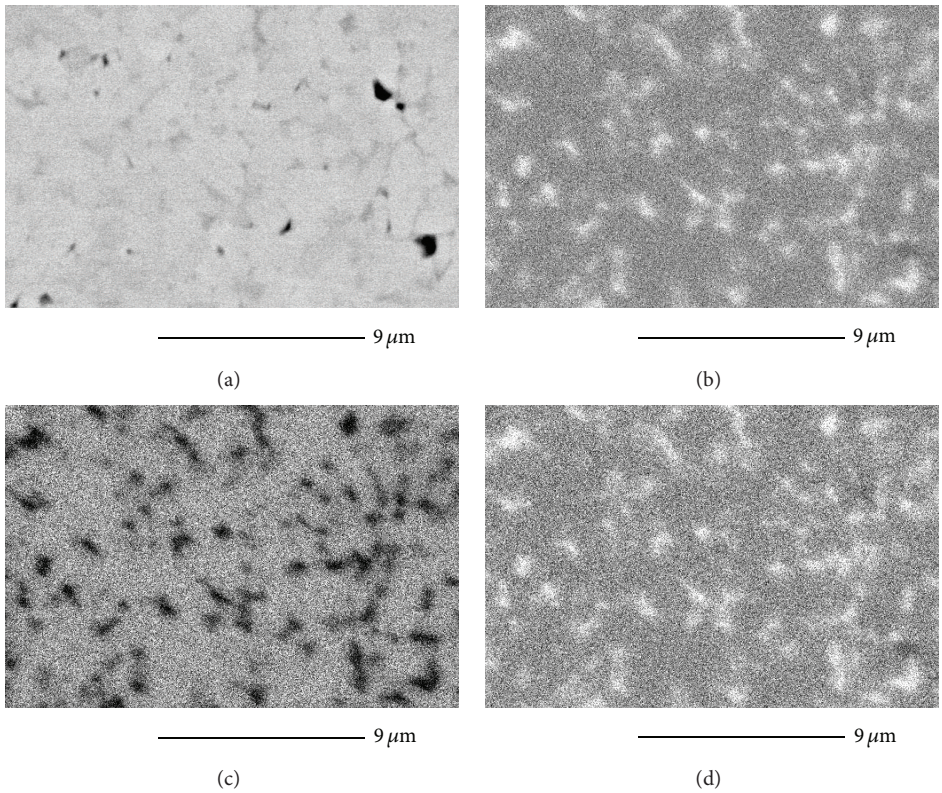

Figure 2: (a) SEM backscatter image and matching EPMA surface elemental mapping for (b) Ba, (c) Sm, and (d) Ti content for the A10-60 sample revealing the Ba- and Ti-rich secondary phase contained within the A10-60 sample. Brighter contrast in (b), (c), and (d) indicates a higher proportion of that element in comparison with darker areas.

display a nonlinear deterioration in Qf and a considerable decrease in τ_{cf} with increasing Sm content. The negative trend in τ_{cf} observed as Sm content increases originates from the contrasting contributions of the positive τ_{cf} Nd-BLnTss analogue and the negative τ_{cf} Sm-BLnTss analogue. The primary driver behind these differing τ_{cf} contributions is attributed to the TiO_6 octahedral tilting resultant from Nd and Sm positioning within the perovskite-like matrix of BLnTss [17].

It was found that Qf significantly deteriorated for $y \geq 0.4$ compositions, and the near-linear slope of τ_{cf} was altered for the same range of compositions (Figure 3(a)). These changes appear to correlate well with the appearance of noncolumnar grain morphologies for these samples (Figures 1(c)-1(d)). Qf begins to degrade as globular grains become apparent, with deleterious effects amplifying with increasing proportions of noncolumnar grain shapes. It is therefore suggested that this degradation in Qf is primarily due to the heterogeneous nature of the phase composition and morphologies in these samples, (i.e., significant variations in composition and a strong deleterious effect of the Ba/Ti-rich second phase). The composition and dielectric characteristics of this Ba/Ti-rich secondary phase are worth investigating further.

The dielectric constant was found to increase slightly with increased Sm content (y-value). Generally speaking, the introduction of smaller isovalent lanthanides (Sm) within the tungsten bronze-type structure results in a lower dielectric permittivity, as the smaller average cell volume decreases the magnitude of potential off-centre Ti ion displacements within the TiO_6 octahedral framework [9]. Accordingly, increased Sm content should lower the dielectric permittivity of BLnTss ceramics. Our results exhibit a different trend, however, with the dielectric permittivity of BLnTss increasing with Sm content. As dielectric permittivity is also highly dependent on the extent to which the sample has undergone densification and crystallisation [1], this is attributed to similar polarisation of both end-members as reported previously [16] and a significant increase in densification observed in the Sm-rich compositions.

With increased sintering time, all A-series samples demonstrated an improved Qf as well as a change in value of τ_{cf} for each composition. An improved linearity of the τ_{cf} transition from positive to negative is also observed with increased sintering time. Improvements in Qf are attributed to an increase in crystallisation, homogenisation of grain size and composition, and a reduction in grain-boundary defects. This is evidenced by improved densification, a reduction in the proportion of globular and needle-like grains, and an observed change in the distribution of the Ba/Ti-rich secondary phase with prolonged sintering. The dielectric constant of the BLnTss ceramics remains almost unchanged as a function of sintering time, suggesting that the samples have been well sintered during the 4-hour sinter and have

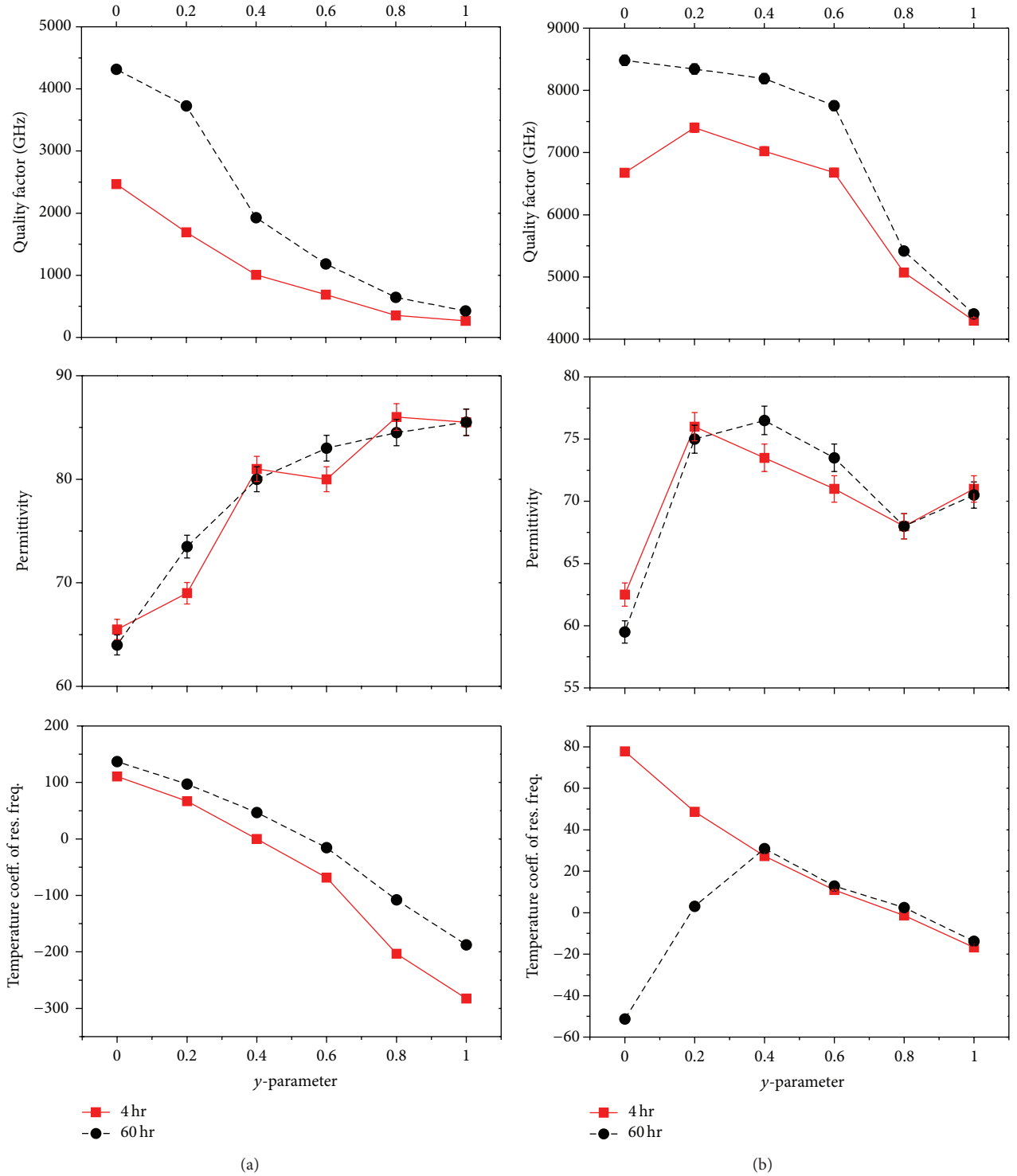

FIGURE 3: Microwave dielectric properties of $Ba_{6-3x}(Nd_{1-y}Sm_y)_{8+2x}Ti_{18}O_{54}$ samples (a) A-Series ($x = 0.33$) and (b) C-Series ($x = 0.67$), sintered for 4 hours (red, solid line) and 60 hours (black, dashed line) at 1375°C. Error bars are displayed for all measurements; however in some cases error range is smaller than data points.

primarily undergone compositional homogenisation over the prolonged sintering period.

C-Series BLnTss samples sintered for 4 hours (Figure 3(b)) also displayed a nonlinear degradation in Qf, a slight increase in ε_r, and a considerable decrease in τ_{cf} with increasing Sm content. Prolonged sintering of C-Series samples was shown to significantly improve crystallisation of Nd-rich samples, while little change was observed for the

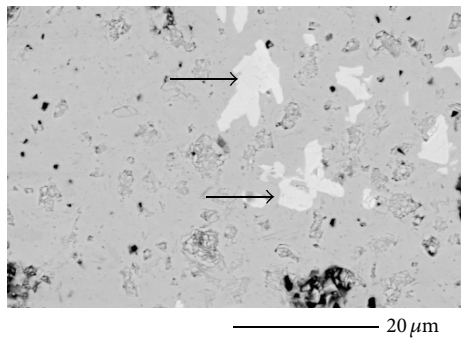

Figure 4: Polished BSE SEM image of C0-60 displaying secondary phase ($Nd_2Ti_2O_7$).

Sm-Rich samples. With prolonged sintering there were two significant changes in dielectric properties observed for the C0-60 and C2-60 samples: a significant improvement in Qf and a distinct change in the τ_{cf} characteristics.

All C-Series samples were initially identified as single phase via XRD. Further investigation via SEM analysis revealed that while the Nd-rich 4-hour samples were single phase, the 60-hour samples displayed segments of distinctly different backscatter contrast (Figure 4) for low Sm content compositions (C0-60 to C6-60). The higher the proportion of Nd in the 60-hour samples, the higher the amount of observed secondary phase. EPMA analysis of these areas confirmed the presence of a secondary phase ($Nd_2Ti_2O_7$).

$Nd_2Ti_2O_7$ has been reported to have a lower permittivity than BLnTss ($\varepsilon_r = 36$), a higher quality factor (Qf = 16,400), and a highly negative temperature coefficient ($\tau_{cf} = -118$ ppm/K) [18]. Improvements in Qf for C-Series Nd-rich samples undergoing extended sintering are therefore attributed to improved crystallisation, a reduction in grain-boundary defects due to increased grain size, improved homogeneity of the main BLnTss phase composition, and excretion of a high-Qf secondary phase. The observed changes in τ_{cf} with prolonged sintering indicate that the highly negative τ_{cf} of $Nd_2Ti_2O_7$ compensates for the positive τ_{cf} of BLnTss, Ln = Nd. Significant improvements in both τ_{cf} and Qf are therefore achieved through the formation of $Nd_2Ti_2O_7$ as a secondary phase.

Prolonged sintering of BLnTss (Ln = Nd) compounds is therefore shown to provide a simplified, one-step method for embedding $Nd_2Ti_2O_7$ into a dense BLnTss matrix. This result effectively enables tuning of the τ_{cf} of BLnTss (Ln = Nd) compounds to near-zero values, whilst improving the density and compositional homogeneity of the primary phase. One multiphase composition with near-zero τ_{cf} was identified for BLnTss prolonged sinter samples; C2-60 with a Qf of 8343, $\varepsilon_r = 75$, and a τ_{cf} of +3.0 ppm/K. While previous reports state that $Ln_2Ti_2O_7$ is one of the precursor compounds of BLnTss [9, 15], there has been no suggestion until now that Nd-BLnTss is metastable for the $x = 0.67$ composition. It is suggested that previous investigations have not revealed the metastable nature of Nd-BLnTss $x = 0.67$, due to their use of microscale reagents and shorter sintering periods. It is proposed that this study, through the use of nanoscale TiO_2 and extended sintering periods, enhanced solid-state reaction characteristics exposing the metastable nature of Nd-BLnT $x = 0.67$.

BLnTss is reported to have the lowest structural strain for the C-Series composition [16], with apparent bond valence values closest to their ideal values for this composition [14]. Through phase segregation of a Nd- and Ti-rich secondary phase, the BLnTss primary phase would move toward a more Ba-rich composition, significantly increasing the global instability index (GII) of the compound based on previous reports [14]. Details of this are worth further investigation.

For B-Series samples, similar trends to the A and C-series samples were observed with regard to improved density and crystallisation with increased Sm content and sintering time. One composition with near-zero τ_{cf} was identified, B8-60 with a Qf of 8044, $\varepsilon_r = 76.5$, and a τ_{cf} of +3.8 ppm/K.

4. Conclusions

$x = 0.33$ ceramics with high Sm content were found to experience a severe degradation of Qf and extreme negative trending of τ_{cf} corresponding with the onset of globular and needle-like grain morphology and the formation of a Ba/Ti-rich secondary phase at BLnTss grain-boundary regions. $x = 0.67$ ceramics with high Nd content were found to exhibit a secondary phase ($Nd_2Ti_2O_7$) upon prolonged sintering which resulted in beneficial changes to Qf and τ_{cf} without affecting ε_r. Two ceramics compositions with near-zero τ_{cf} were synthesised; $x = 0.5$, $y = 0.8$ (Qf = 8044, $\varepsilon_r = 76.5$, and $\tau_{cf} = +3.8$ ppm/K) and $x = 0.67$, $y = 0.2$ (Qf = 8343, $\varepsilon_r = 75$, and $\tau_{cf} = +3.0$ ppm/K).

Acknowledgments

Amanda L. Snashall, Yun Liu, and Ray L. Withers thank the Australian Research Council for financial support in the form of ARC Linkage Grants. Amanda L. Snashall is grateful for the funding supplied via her Australian Postgraduate Award Industry scholarship.

References

[1] M. T. Sebastian, *Dielectric Ceramics For Wireless Communication*, 1st edition, 2008.

[2] R. L. Bolton, *Temperature Compensating Ceramic Capacitors in the System Barium Oxide-Rare Earth Oxide-Titania*, 1968.

[3] A. M. Gens, M. B. Varfolomeev, V. S. Kostomarov, and S. S. Korovin, "Crystal-chemical and electrophysical properties of complex titanates of rare earth elements and barium," *Zhurnal Neorganicheskoi Khimii*, vol. 26, no. 4, pp. 896–898, 1981.

[4] H. Ohsato, "Research and development of microwave dielectric ceramics for wireless communications," *Journal of the Ceramic Society of Japan*, vol. 113, no. 1323, pp. 703–711, 2005.

[5] D. Suvorov, M. Valant, and D. Kolar, "The role of dopants in tailoring the microwave properties of $Ba_{6-3x}Ln_{8+2x}Ti_{18}O_{54}$ R = (La-Gd) Ceramics," *Journal of Materials Science*, vol. 32, no. 24, pp. 6483–6488, 1997.

[6] M. Valant, D. Suvorov, and C. J. Rawn, "Intrinsic reasons for variations in dielectric properties of $Ba_{6-3x}Ln_{8+2x}Ti_{18}O_{54}$ R = (La-Gd) solid solutions," *Japanese Journal of Applied Physics*, vol. 38, no. 5, pp. 2820–2826, 1999.

[7] H. Ohsato, J. Sugino, A. Komura, S. Nishigaki, and T. Okuda, "Microwave dielectric properties of $Ba_4(Nd_{28/3-y}R_y)Ti_{18}O_{54}$ (R = Eu, Dy, Ho, Er and Yb) solid solutions," *Japanese Journal of Applied Physics*, vol. 38, no. 9, pp. 5625–5628, 1999.

[8] T. Negas and P. K. Davies, "Influence of chemistry and processing on the electrical properties of $Ba_{6-3x}Ln_{8+2x}Ti_{18}O_{54}$ solid solutions," *Ceramic Transactions*, vol. 53, pp. 179–196, 1995.

[9] S.-F. Wang, Y.-F. Hsu, Y.-R. Wang et al., "Densification, microstructural evolution and dielectric properties of $Ba_{6-3x}(Sm_{1-y}Nd_y)_{8+2x}$ $Ti_{18}O_{54}$ microwave ceramics," *Journal of the European Ceramic Society*, vol. 26, no. 9, pp. 1629–1635, 2006.

[10] Y. Li and X. M. Chen, "Effects of sintering conditions on microstructures and microwave dielectric properties of $Ba_{6-3x}(Sm_{1-y}Nd_y)_{8+2x}$ $Ti_{18}O_{54}$ ceramics (x=2/3)," *Journal of the European Ceramic Society*, vol. 22, no. 5, pp. 715–719, 2002.

[11] K. M. Cruickshank, X. Jing, G. Wood, E. E. Lachowski, and A. R. West, "Barium neodymium titanate electroceramics: phase equilibria studies of $Ba_{6-3x}Ln_{8+2x}Ti_{18}O_{54}$ solid solution," *Journal of the American Ceramic Society*, vol. 79, no. 6, pp. 1605–1610, 1996.

[12] L. Zhang, X. M. Chen, N. Qin, and X. Q. Liu, "Upper limit of x in $Ba_{6-3x}Ln_{8+2x}Ti_{18}O_{54}$ new tungsten bronze solid solution," *Journal of the European Ceramic Society*, vol. 27, no. 8-9, pp. 3011–3016, 2007.

[13] H. Ohsato, T. Ohhashi, S. Nishigaki, T. Okuda, K. Sumiya, and S. Suzuki, "Formation of solid solutions of new tungsten bronze-type microwave dielectric compounds $Ba_{6-3x}Ln_{8+2x}Ti_{18}O_{54}$ (R = neodymium and samarium, $0 < X < 1$)," *Japanese Journal of Applied Physics*, vol. 32, no. 9, pp. 4323–4326, 1993.

[14] A. L. Snashall, L. Norén, Y. Liu, T. Yamashita, F. Brink, and R. L. Withers, "Phase analysis and microwave dielectric properties of $BaO\text{-}Nd_2O_3\text{-}5TiO_2$ composite ceramics using variable size TiO_2 reagents," *Ceramics International*, vol. 38, no. 1, pp. S153–S157, 2012.

[15] A. G. Belous, O. V. Ovchar, M. Valant, and D. Suvorov, "Solid-state reaction mechanism for the formation of $Ba_{6-x}Ln_{8+2x/3}Ti_{18}O_{54}$ (Ln = Nd, Sm) solid solutions," *Journal of Materials Research*, vol. 16, no. 8, pp. 2350–2356, 2001.

[16] H. Ohsato, "Science of tungstenbronze-type like $Ba_{6-3x}Ln_{8+2x}Ti_{18}O_{54}$ (R = rare earth) microwave dielectric solid solutions," *Journal of the European Ceramic Society*, vol. 21, no. 15, pp. 2703–2711, 2001.

[17] I. M. Reaney, "Effect of octahedral tilt transitions on the properties of perovskites and related materials," *Ferroelectrics*, vol. 222, no. 1–4, pp. 401–410, 1999.

[18] J. Takahashi, K. Kageyama, and K. Kodaira, "Microwave dielectric properties of lanthanide titanate ceramics," *Japanese Journal of Applied Physics*, vol. 32, no. 9, pp. 4327–4331, 1993.